

Multiple Time- and Space-Scale Comparisons of ATLAS Buoy Rain Gauge Measurements with TRMM Satellite Precipitation Measurements*

YOLANDE L. SERRA

Joint Institute for the Study of the Atmosphere and Ocean, University of Washington, Seattle, Washington

MICHAEL J. MCPHADEN

NOAA/Pacific Marine Environmental Laboratory, Seattle, Washington

(Manuscript received 10 May 2002, in final form 26 February 2003)

ABSTRACT

This study compares the Tropical Rainfall Measuring Mission (TRMM) microwave imager (TMI) and precipitation radar (PR) rainfall measurements to self-siphoning rain gauge data from 14 open-ocean buoys located in heavy-rain areas of the tropical Pacific and Atlantic Oceans. These 14 buoys are part of the Tropical Atmosphere–Ocean (TAO) array and Pilot Research Moored Array in the Tropical Atlantic (PIRATA). Differences between buoy and TRMM monthly and seasonal rainfall accumulations are calculated from satellite data within $0.1^\circ \times 0.1^\circ$ – $5.0^\circ \times 5.0^\circ$ square areas centered on the buoys. Taking into account current best estimates of sampling and instrumental errors, mean differences between the buoy and TMI rainfall are not significant at the 95% confidence level, assuming no wind-induced undercatch by the buoy gauges. Mean differences between the buoy and PR monthly and seasonal accumulations for these spatial scales suggest that the PR underestimates these accumulations by about 30% in comparison with the buoys. If the buoy rain rates are corrected for wind-induced undercatch, TMI accumulations fall systematically and significantly below buoy values, with underestimates of up to 22% for both monthly and seasonal data. Also the PR underestimates, relative to wind-corrected buoy values, increase to up to 40% for both monthly and seasonal data. Regional and rain-rate dependencies of these comparisons are also investigated.

1. Introduction

The amount and spatial distribution of precipitation in the Tropics constitute vital information for understanding climate variability. Convective heating is the primary means by which the sun's energy is distributed to the atmosphere to drive both local- and large-scale circulations. Latent heat released within precipitating systems accounts for 75% of the convective heat transport in the atmosphere. Of this heating, approximately two-thirds, or 50% of the global convective heat transport in the atmosphere, is produced by tropical systems. Long-term variability in tropical rainfall affects weather around the globe through teleconnections, such as those associated with ENSO. Precipitating systems also affect the buoyancy and momentum budgets of the tropical

upper ocean, with most of the Tropics consisting of ocean, rather than land, surfaces.

The Tropical Rainfall Measuring Mission (TRMM) satellite was launched in late 1997 as a 3-yr project to obtain measurements of tropical precipitation with long-term $5^\circ \times 5^\circ$ monthly sampling errors of less than 10% (Simpson et al. 1996). The TRMM satellite sensor package consists of a spaceborne precipitation radar (PR), a multichannel microwave imager (TMI), and a five-channel visible–infrared radiometer (VIRS). Ground validation of TRMM rainfall products is crucial for improving satellite retrieval algorithms beyond the current state of knowledge, and to achieve the goal of 10% rainfall uncertainty for the $5^\circ \times 5^\circ$ monthly data. Whereas radar and rain gauge networks are available across global land areas, open-ocean validation relies on short-term datasets from ship-based process studies. Other longer-term datasets are available from islands and atolls. However, these data are potentially contaminated by land-heating effects. In addition, these sites are not necessarily located in the regions of interest.

The Tropical Atmosphere–Ocean (TAO) and Triangle Trans-Ocean Buoy Network (TRITON) buoy array consists of approximately 70 Autonomous Temperature

* Joint Institute for the Study of the Atmosphere and Ocean Contribution Number 919 and NOAA/Pacific Marine Environmental Laboratory Contribution Number 2471.

Corresponding author address: Dr. Yolande Serra, Joint Institute for the Study of Atmosphere and Ocean, Box 357941, University of Washington, Seattle, WA 98195-7941.
E-mail: yolande.serra@noaa.gov

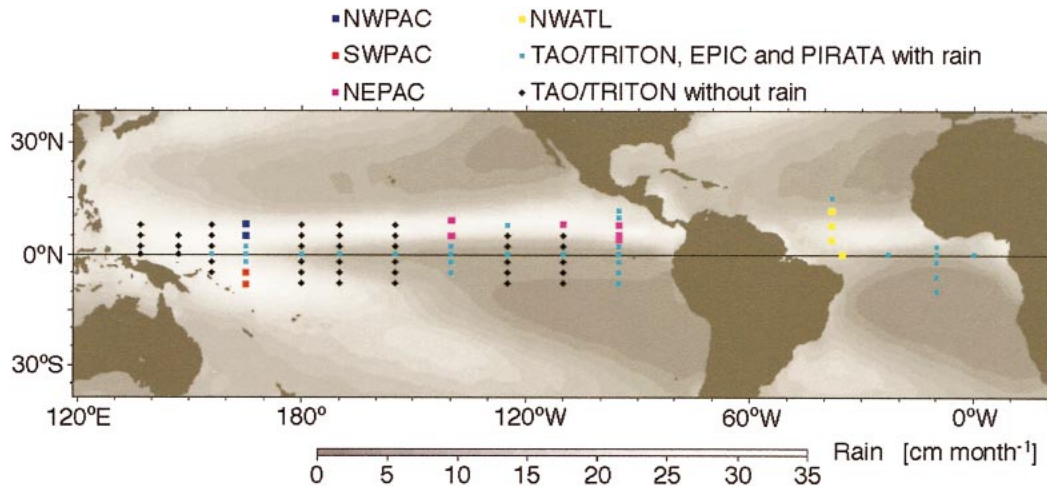


FIG. 1. The TAO–TRITON, Eastern Pacific Investigation of Climate (EPIC), and PIRATA buoys: moorings with rain gauges (colored square symbols) and moorings without gauges (black diamonds). Matching large, colored squares classify the rain gauges into four heavy-rain areas discussed in the text. Also shown is the 1979–2000 2.5° rainfall climatological data from the CMAP product.

Line Acquisition System (ATLAS) and TRITON buoys between 8°S and 8°N, 137°E and 95°W across the tropical Pacific Ocean (McPhaden et al. 1998). Additional buoys at 3.5°, 10°, and 12°N along 95°W were deployed in late 1999 as part of the Pan-American Climate Studies (PACS) program (Cronin et al. 2002). The Pilot Research Moored Array in the Tropical Atlantic (PIRATA) is an array of 12 ATLAS buoys in the tropical Atlantic Ocean (Servain et al. 1998). Currently, 28 ATLAS moorings in the TAO–TRITON array have self-siphoning rain gauges, while all PIRATA ATLAS moorings are equipped with such gauges.

The objective of this study is to validate the TRMM satellite rainfall measurements against the TAO/PIRATA ATLAS buoy measurements using a subset of 14 buoys located within heavy-rain areas of the tropical Pacific and Atlantic. These 14 sites were chosen because they provide the largest number of heavy-rain events and, thus, the best statistics for a rainfall comparison study. Our analysis includes monthly and seasonal time periods and, for the satellite data, six areas ranging from 0.1° to 5.0° squares that are centered on the buoys. Separate comparisons of percent time-raining, rain rate, and accumulation are presented in order to determine the affect of the satellite sampling on measuring the frequency and intensity of rain.

2. The data

Figure 1 shows the locations of the buoys within the TAO–TRITON and PIRATA arrays, highlighting the 14 TAO and PIRATA buoys used for this study (large colored squares). All other TAO and PIRATA buoys with rain gauges are also noted (small cyan squares), as well as those without rain gauges (small black diamonds). Average rainfall at 2.5° resolution for 1979–2000 from

the National Oceanic and Atmospheric Administration (NOAA) National Centers for Environmental Prediction (NCEP) Climate Prediction Center (CPC) Merged Analysis of Precipitation (CMAP) (Xie and Arkin 1997) is also shown to indicate the climatological rainfall in the vicinity of the data compared in this study (gray contours).

a. TRMM

The TRMM satellite was launched in October 1997, with the first data returns in December 1997 (Kummerow et al. 1998). Version 5 of TRMM 2A12 (TMI) and 2A25 (PR) datasets, covering December 1997 through December 2000, are used in this study to compare with the TAO and PIRATA ATLAS buoy measurements. The 2A12 and 2A25 datasets provide surface rain rate (mm h^{-1}) for individual TMI and PR footprints, which we then average over a selected area and time period to compare with the buoy values. The information on the TMI and PR swath widths, resolution, and sensitivity provided here is applicable to only those data collected prior to August 2002, after which time the TRMM satellite was moved to a higher orbit to extend the lifetime of the data collection period.

The TMI has an elliptical footprint ranging from 63 km \times 37 km for the 10.65-GHz channel, to 7 km \times 5 km for the 85.5-GHz channel. There are 208 (26) footprints per scan for the 85.5-GHz (10.65 GHz) channel, where a scan is an arc approximately 760 km along the cross-track direction. One orbit consists of approximately 3000 scans. The satellite has an approximate 7-day repeat cycle and covers all longitudes between 40°S and 40°N within this time. Surface rain rate for the orbital TMI data is provided at the resolution of the 85.5-GHz channel, 7 km \times 5 km. However, the move-

ment of the satellite and scan geometry result in a true resolution for these data of approximately 50 km^2 , and a threshold of about 0.5 mm h^{-1} (C. Kummerow 2001, personal communication).

The TRMM PR has a circular footprint that is 4.3 km in diameter, and a swath width of 215 km. The PR has a threshold of 15–20 dBZ, or about $0.2\text{--}0.4 \text{ mm h}^{-1}$ (Schumacher and Houze 2000). Surface rain rate for the orbital PR data is provided at the spatial resolution of the radar footprint.

b. ATLAS self-siphoning rain gauges

ATLAS buoys are designed and assembled at the NOAA/Pacific Marine Environmental Laboratory (PMEL) for the TAO–TRITON and PIRATA arrays. Standard ATLAS measurements have been collected since 1984 and include 3-m air temperature and relative humidity, 4-m wind speed and direction, and ocean temperatures at 11 depths from 1 to 500 m. New next-generation ATLAS buoys, deployed at selected locations since 1997, can additionally measure barometric pressure, shortwave and longwave radiation, precipitation, and salinity.

The next-generation ATLAS buoys measure precipitation using R. M. Young Company Model 50203-34 self-siphoning rain gauges (hereinafter referred to as rain gauges or simply gauges) mounted 3.5 m above the ocean surface. The instruments capture rain water and funnel it into a fill tube with a 500-ml capacity. The amount of water is measured by capacitance, which is a function of the water volume in the tube. The fill tube automatically siphons at 500 ml. The instrument resolution is on the order of a few tens of millimeters and is independent of rain rate, but it does depend, to a small degree, on water volume in the tube.

A complete description of the rain gauges used on ATLAS buoys and their error characteristics is given in Serra et al. (2001, hereinafter S01). Their results indicate that the random error in 10-min rain rates is 0.4 mm h^{-1} . The data used for the present study are based on hourly rain rates, which are estimated to have random errors on the order of 0.15 mm h^{-1} (assuming the errors are normally distributed so that they reduce like $1/\sqrt{N}$). The largest systematic error for these instruments is due to wind effects, which may bias the rain gauge estimates, low by about 10%–50% for wind speeds encountered at ATLAS buoys. These estimates are similar to those of Groisman and Legates (1994), who estimate that monthly precipitation measured from rain gauges in the United States can be underestimated by roughly 5%–40%. They find that errors increase from south to north in the United States because of snowfall, which is more susceptible to wind-induced errors than rain. A wind speed correction is provided in S01, based on Koschmieder (1934). Because this correction is not specific to the rain gauges on the buoys, we focus on the uncorrected buoy data for these comparisons. The effects

of the wind speed correction on the results are significant, however, and are presented in section 7b.

3. Monthly-to-interannual variability of rainfall in the tropical Pacific and Atlantic

Time series of monthly rainfall accumulation from the TRMM and buoy data are presented in Fig. 2 for the northwest tropical Pacific (NWPAC), southwest tropical Pacific (SWPAC), northeast tropical Pacific (NEPAC), and northwest tropical Atlantic (NWATL) (section 4, Fig. 1). The CMAP (Xie and Arkin 1997) 2.5° rainfall product for the December 1997–December 2000 time period and the CMAP climatology, based on the 1979–2000 time period, are also shown in the figure for comparison. Rainfall from the closest CMAP grids to the 14 buoy locations were averaged and then combined to get the four regional averages shown. The TMI and PR data are presented as 2.5° monthly accumulations to match the CMAP data resolution.

The phase of the seasonal cycle in the NEPAC region differs among the buoy sites included in this region, so we have isolated a group of three buoys with a similar timing of seasonal variations for the purpose of this figure. The NEPAC-South data shown in Fig. 2c consist of buoy data from 5° and 3.5°N along 95°W , and from 5°N along 140°W . Similarly, the phase of the seasonal cycle for the NWATL sites also differs between the northern (12° and 8°N , 38°W) and southern (4°N , 38°W and 0° , 35°W) sites. Figure 2d shows an average of the data from the northern sites only (NWATL North). Similar agreement among the various platforms shown in Fig. 2 is observed for all the NEPAC and NWATL time series comparisons.

Rainfall variability in the tropical north Pacific and Atlantic is dominated by the seasonal migration of the inter tropical convergence zone (ITCZ). In boreal winter the ITCZ is closest to the equator, resulting in precipitation minima in the tropical north Pacific and Atlantic at this time (Figs 2a,c,d). The ITCZ moves northward, beginning around March, reaching its northernmost position ($\sim 10^\circ\text{N}$) in the late boreal summer to early autumn. The migration of the ITCZ is evident in the boreal spring precipitation maxima in the NEPAC-South (Fig. 2c), and in the late summer maximum in the NWATL-North (Fig. 2d). Along 165°E (the eastern edge of the warm pool during normal years), the annual cycle in precipitation is weaker than in the eastern Pacific and western Atlantic, and is determined by changes in strength of the ITCZ north of the equator and the South Pacific convergence zone (SPCZ) south of the equator. The ITCZ and SPCZ are most active during their respective hemisphere's summer season, indicated by the out-of-phase relationship between the maxima in the Northern and Southern Hemispheres (Figs. 2a,b).

Deviations from climatology related to the 1997–98 El Niño, which occurred from roughly March of 1997 to March 1998, are also observed. The anomalously dry

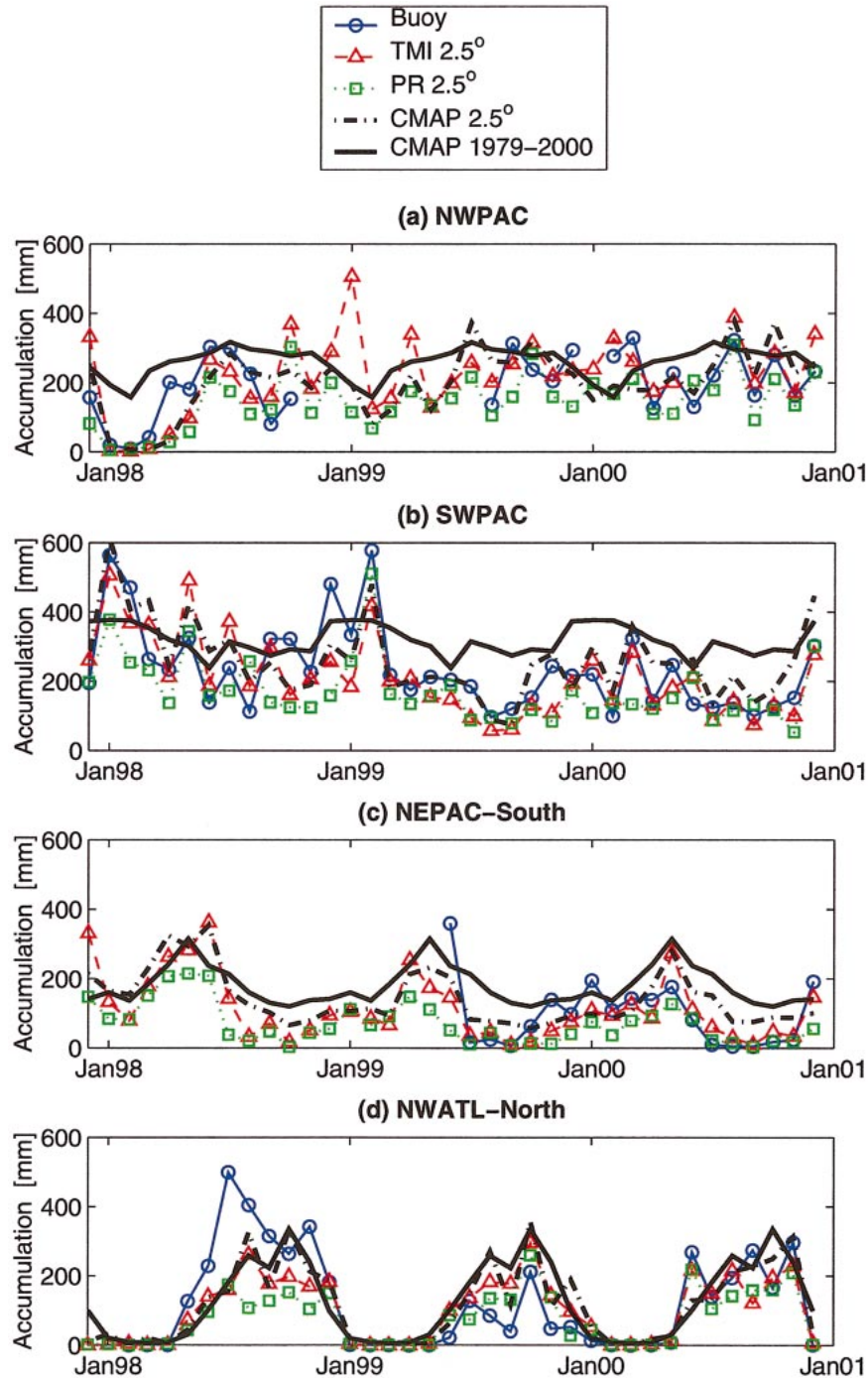


FIG. 2. Time series of buoy and TRMM monthly rainfall accumulations for the (a) NWPAC, (b) SWPAC, (c) NEPAC-South, and (d) NWATL-North; and the CMAP 2.5°-resolution monthly accumulations for these same regions and CMAP 1979–2000 climatology.

conditions in the NWPAC (Fig. 2a) and the somewhat anomalously wet conditions in the SWPAC (Fig. 2b) in early 1998 are a consequence of the equatorward shifts of the ITCZ and SPCZ. There is also a hint of wetter-than-normal conditions in the NEPAC-South region for

the TMI, buoy, and CMAP data (Fig. 2c). No effect of the El Niño is seen in the Atlantic rainfall (Fig. 2d).

A rapid transition to La Niña conditions in the central equatorial Pacific in May–June 1998 (McPhaden 1999) is coincident with relatively dry conditions in the

NWPAC during most all of 1998 (with the exception of the TRMM data later in the year), and the spring of both 1999 and 2000 (Fig. 2a). The SST anomalies indicate that La Niña conditions were strongest from May 1998 to 1999, with Niño-3, -3.4, and -4 indices indicating that weaker La Niña conditions persisted throughout 2000 and into the early part of 2001 (U.S. Department of Commerce 2002). Dry conditions are also observed in the SWPAC from March 1999–December 2000, and are more pronounced than those observed in the NWPAC (Fig. 2b). Data from the NEPAC-South indicate that somewhat dry conditions existed during the rainy season in this region for 1998–2000 (Fig. 2c). Convection in the NWATL-North shows little overall change due to La Niña, with only a hint of drying during the 1999 wet season (Fig. 2d).

The patterns of rainfall variability over the 37-month time period shown in Fig. 2 are qualitatively similar among the buoy, TMI, and PR data. The buoy and the 2.5°-resolution TMI and PR data also agree reasonably well with the CMAP 2.5° monthly rainfall product. However, it is evident that the PR values tend to be lower than those of the buoys, while the TMI falls both above and below buoy values at times, with differences being on the order of the natural variability of rainfall implied by the patterns in the time series. Uncertainties in rainfall accumulation of these magnitudes have important consequences for calculations of hydrological budgets, ocean mixed-layer stability in the Tropics, and other physical processes that require accurate precipitation measurements. While the magnitude of the natural variability of rainfall is a limiting factor in assessing the agreement among various rainfall products, we attempt to quantify the agreement between the buoy and TRMM measurements using multiple buoys and a long data record to reduce the scatter in such comparisons.

4. Comparison methodology

a. Definition of mean quantities

In order to quantify the differences between the buoy and satellite rainfall measurements exemplified in Fig. 2, we consider not only rain accumulation, but also the frequency (i.e., percent time-raining) and intensity (i.e., conditional rain rate) of rain. Percent time-raining is defined for the buoys as the percent of hourly data samples in a month or season with rain rates greater than 0.5 mm h⁻¹. For the satellite, the percent time-raining is estimated as the percent of footprints within a given area and over a month or season with rain rates greater than 0.5 mm h⁻¹. Conditional rain rate is the subset of all buoy or satellite rain-rate data with rates greater than 0.5 mm h⁻¹. A threshold of 0.5 mm h⁻¹ is chosen to roughly match the sensitivity of the satellite instruments.

Rain rate is in units of millimeters per hour for each satellite footprint, while accumulation is measured by the buoy rain gauges and is differenced to get hourly

TABLE 1. Mean of monthly percent time-raining, conditional rain rate, and accumulation for the buoy gauges, as well as for the 2.5° TMI and PR data. Means are based on months with nonzero percent time-raining from Dec 1997 to Dec 2000.

	P (%)	R_c (mm h ⁻¹)	R (mm h ⁻¹)	A (mm)
Buoy	8.9	2.8	0.27	200
TMI 2.5°	8.9	2.3	0.24	180
PR 2.5°	5.7	2.5	0.17	120

rain rates. Satellite accumulation is derived from conditional rain rate and percent time-raining, using the simple relation,

$$A = (P/100 \times R_c)\Delta T. \quad (1)$$

If T is in units of hours, then R_c is the average conditional rain rate for time ΔT in units of millimeters per hour, P is the percent time-raining for time ΔT , and A is accumulation over time ΔT in millimeters. Alternatively, we could use the average rain rate, including zero values, equivalent to the expression in parentheses in (1), and simply multiply by the number of hours in a month or season to get monthly or seasonal accumulation. However, this would not allow us to compare the frequency or intensity of events measured by the buoy and satellite.

Table 1 shows the overall mean values of the rainfall parameters for buoy gauges, as well as for the 2.5° TMI and PR data. Mean values from only one of the six satellite-averaging regions are shown in the table for simplicity. The 2.5° region is selected because, as will be shown, it compares well with the buoy data and is used for subsequent calculations in later sections.

b. Definition of errors

In the present study we are interested in determining if there is a significant difference between the satellite and gauge estimates of rainfall parameters collected over a 3-yr time period. We have chosen to compare both monthly and seasonal rainfall parameters and, for the satellite, space scales [on the order of a satellite footprint (0.1° × 0.1°)], with the scale for which TRMM rainfall is expected to have a long-term monthly accuracy of 10% (5.0° × 5.0°). To minimize errors in the satellite and gauge estimates of monthly and seasonal means, we select locations with the greatest number of rain events. The heaviest areas of rain in the tropical Pacific and Atlantic are the warm pool in the NWPAC, the SPCZ in the SWPAC, and the ITCZ in the NEPAC and NWATL. Fourteen buoy sites are located within these heavy-rain areas and are used in this study: 5° and 8°N, 165°E (NWPAC; Fig. 1, blue squares); 5° and 8°S, 165°E (SWPAC; Fig. 1, red squares); 5° and 9°N, 140°W, 8°N, 110°W, and 3.5°, 5°, and 8°N, 95°W (NEPAC; Fig. 1, magenta squares); and 0°, 35°W and 4°, 8°, and 12°N, 38°W (NWATL; Fig. 1, yellow squares).

These sites have at least 6 months of data, and 1 month exceeding 200 mm of rainfall.

The difference between the satellite and buoy monthly or seasonal rain rates is defined as

$$\Delta = \langle R_s \rangle - \langle R_g \rangle, \quad (2)$$

where R_s is the satellite rain-rate measurement for a given footprint, R_g is the hourly gauge measurement, and the brackets represent the average over a month or season and, for the satellite, an area centered on the gauge within the range of scales noted above. Mean rain rates for the buoys and satellite are calculated based on lognormal statistics. Kedem et al. (1990) demonstrate that an accurate mean rain rate can be obtained using a lognormal distribution for a variety of space–time sampling schemes, even if all of the rain-rate data are not completely independent, as is the case for both the hourly buoy and satellite footprint measurements.

The expected error in the differences between buoy and satellite rain-rate measurements from (2) can be expressed as

$$\sigma_\Delta = \sqrt{\sigma_{\text{samp}}^2 + \sigma_{\text{err},s}^2 + \sigma_{\text{err},g}^2}, \quad (3)$$

where σ_{samp} is the sampling error, and $\sigma_{\text{err},s}$ and $\sigma_{\text{err},g}$ are the random measurement errors for the satellite and gauge, respectively. The sampling errors include the natural variability of rain as well as the error associated with the fact that the satellite and gauge averages are based on different time- and space scales. Equation (3) assumes that the random errors for the gauge and satellite are uncorrelated. As will be shown in section 7b, this is likely a good assumption.

We are primarily concerned with the expected magnitude of the monthly and seasonal mean difference $\langle \Delta \rangle$, the standard error of which is defined as

$$\sigma_{\langle \Delta \rangle} = \sigma_\Delta / \sqrt{N} = \sqrt{(\sigma_{\text{samp}}^2 + \sigma_{\text{err},s}^2 + \sigma_{\text{err},g}^2) / N}, \quad (4)$$

where N is the number of comparison months or seasons. Seasonal means are only computed for seasons with all 3 months of data. The monthly and seasonal differences have a normal distribution permitting the use of normal statistics for determining the mean and standard errors. In the remainder of this section we will show that, while estimates of σ_Δ can be quite large for a given month or season, estimates of $\sigma_{\langle \Delta \rangle}$ are less than a few percent for all but the smallest satellite-averaging regions.

We use the method of Bell et al. (1990, hereafter B90) to estimate the magnitude of random retrieval errors in monthly averaged satellite rain rates for six areas ranging from $0.1^\circ \times 0.1^\circ$ to $5.0^\circ \times 5.0^\circ$, corresponding to the areas used for the comparisons in section 5. B90 define the area-averaged rain rate within a satellite field of view (FOV; or footprint) as $\hat{R}_{\text{FOV}} = (1 + \epsilon)R_{\text{FOV}}$, where R_{FOV} is the estimated rain rate from the satellite and \hat{R}_{FOV} is the true mean rain rate. Their calculations assume that retrieval errors are unbiased over the time- and space scales considered, such that $\langle \epsilon \rangle = 0$. From their Eq. (A7), the retrieval error is then defined as

$$\sigma_{\text{err},s}^2 = \frac{\langle \epsilon_i^2 \rangle \langle R_{\text{FOV}}^2 \rangle}{N_{\text{FOV}}}, \quad (5)$$

where N_{FOV} is the number of satellite footprints within a given area over a month or season. As in B90, we assume $\langle \epsilon_i^2 \rangle = 1$, or, that individual retrievals are accurate to a factor of 2. In addition, we use their value of $5 \text{ mm}^2 \text{ h}^{-2}$ for the monthly spatial variance of rain rate over the area of a typical satellite footprint $\langle R_{\text{FOV}}^2 \rangle$, based on the Global Atlantic Research Program (GARP) Atlantic Tropical Experiment (GATE) data. Table 2 lists the typical number of satellite footprints through each of the square areas within a month and season. Substituting the above values and those in Table 2 for monthly data into (5), and dividing by a monthly mean rain rate of 0.3 mm h^{-1} (based on buoy data from Table 1), our calculations suggest that retrieval errors range from 84% of the monthly mean rain rate for $0.1^\circ \times 0.1^\circ$ areas, down to 2% (same as B90 results) for $5.0^\circ \times 5.0^\circ$ areas. Extending the averaging time to 90 instead of 30 days, we estimate that these errors would approximately be halved for seasonal mean rain rates.

Based on the results of S01, we estimate that random errors in rain rate from ATLAS gauges ($\sigma_{\text{err},g}$) are negligible over time periods of a month or season, with the possible exception of wind-induced errors. As already mentioned, these errors can be significant, but are not specifically known for ATLAS gauges. Therefore, for the purpose of estimating $\sigma_{\langle \Delta \rangle}$, we will ignore this error until section 7b. It should be kept in mind that wind-induced errors can only reduce gauge rainfall averages, making them a lower bound on the true values observed at the buoys.

To estimate the expected magnitude of the sampling error σ_{samp} in (4) we refer to Bell and Kundu (2003, hereafter BK03). Using a theoretical statistical model with parameters based on radar data from GATE and the Tropical Ocean and Global Atmosphere (TOGA) Coupled Ocean–Atmosphere Response Experiment (COARE), BK03 estimate σ_{samp} for several satellite–gauge comparison scenarios. The one of relevance to this study is the case of a satellite passing over a single rain gauge once per day over the period of a month. Relative sampling errors based on the GATE data are calculated as a function of area and are $\geq 60\%$ for areas up to $0.5^\circ \times 0.5^\circ$, $\sim 40\%$ for $1^\circ \times 1^\circ$ areas, and asymptotically approach $\sim 30\%$ for areas of $2.5^\circ \times 2.5^\circ$ or larger. Relative sampling errors based on the TOGA COARE rainfall statistics are anywhere from a few percent to 10% higher than the GATE sampling errors, depending on the radar and data time period selected (T. L. Bell 2002, personal communication).

As seen in Table 1, on average, 8%–9% of the TMI footprints and buoy hourly data contain rain over 1 month for the months used in this study, while about 6% of the PR footprints contain rain for these months (also see Fig. 7a). Table 2 shows the typical number of orbits passing over the buoys in a month, the typical

TABLE 2. The typical number of satellite footprints within an averaging area is listed for monthly and seasonal time periods, along with the number of buoy comparison months and seasons, respectively. The typical number of orbits in a month, and the fraction of those orbits covering the entire area and one-half of the area around the buoys are also noted.

Area linear dimension	Typical number of footprints in a month	Number of comparison months	Typical number of footprints in a season	Number of comparison seasons	Typical number of orbits in a month	Typical fraction of orbits covering area	Typical fraction of orbits covering one-half of area
0.1°	78	177	235	59	2	1.0	1.0
	57	136	171	58		1.0	1.0
0.2°	303	196	910	62	2	1.0	1.0
	230	178	690	62		1.0	1.0
0.5°	1930	213	5740	64	5	1.0	1.0
	1440	208	4300	66		1.0	1.0
1.0°	7700	225	23 100	65	9	1.0	1.0
	5760	226	17 400	67		0.1	1.0
2.5°	43 300	229	144 000	65	22	0.7	1.0
	36 100	234	108 000	69		0	0.5
5.0°	193 000	230	577 000	65	42	0	0.8
	144 000	234	429 000	69		0	0

fraction of those overpasses that cover the entire comparison area, and the typical number that cover one-half of this area. The information in Table 2 was estimated using the TRMM Overview Finder (<http://tsdis02.nascom.nasa.gov/overflight/>). Note that the 5° × 5° area is wider than the usable area of the satellite swath, such that no orbits completely contain it. The percent of data with rain in any given month and the number of satellite passes over the buoys in 1 month are pointed out here to emphasize the factors contributing to the sampling errors in this study. The BK03 model is specifically designed to address the sampling errors associated with undersampling a given area and/or time period. However, the GATE and COARE radar data used to estimate characteristic time- and space scales of rainfall in their model have a horizontal resolution of 4 and 2 km, respectively, and have less than 1 month of continuous observations. Thus, rainfall variability at smaller spatial scales and longer timescales, such as measured by 1 month or longer of gauge data, are not represented by this model. The BK03 results also imply that spatial and temporal scales of rainfall variability vary significantly with region and type of rain. Thus, estimates of the sampling error should ideally be calculated for each region and as a function of rain rate for our comparison months. Because we are unable to obtain, or estimate from our data, spatial and temporal statistics of rainfall for all the regions and types of rain encompassed by our comparison months, we have chosen to double the BK03 errors to estimate σ_{samp} .

Using the estimated satellite retrieval errors and sampling errors, as discussed above, and ignoring the wind-induced errors from the rain gauge, until section 7b, we calculate the expected total standard error in the mean difference $\sigma_{(\Delta)}$ defined in (4) for the range of spatial averages presented in this study. Table 2 shows the number of comparison months and seasons for each averaging area. Table 3 provides the results of these calculations for monthly and seasonal data relative to an 0.3 mm h⁻¹ mean rain rate. The seasonal values are calculated, assuming satellite retrieval errors are one-half of the monthly values and sampling errors remain the same as for monthly comparisons. If the observed differences exceed the standard errors in Table 3, our assumption of no mean bias in the retrieval and/or sampling errors would be violated. The values in Table 3 suggest that significant differences (biases) between the satellite and buoys greater than about 15% should be evident from the monthly comparisons in this study for all spatial scales, and that differences greater than about 20% should be evident for the seasonal comparisons. Seasonal comparisons have larger uncertainties than the monthly comparisons simply because there are fewer seasons than months to compare.

An empirical estimate of (4), based on the data used in this study, is defined as

$$\tilde{\sigma}_{(\Delta)} = \sqrt{(\sigma_g^2 + \sigma_s^2)/N}, \quad (6)$$

TABLE 3. Total error in the bias between the satellite and buoy as estimated from (4) for unconditional rain rate ($\sigma_{(\Delta)}$) and from (6) for percent time-raining (P), conditional rain rate (R_c), and accumulation (A). Values of $\sigma_{(\Delta)}$ are based on B90 and BK03. Only the range of $\bar{\sigma}_{(\Delta)}$ for P , R_c , and A is shown. See text for details.

Area linear dimension		Relative error in monthly bias (%)		Relative error in seasonal bias (%)	
		$\sigma_{(\Delta)}$	$\bar{\sigma}_{(\Delta)}$	$\sigma_{(\Delta)}$	$\bar{\sigma}_{(\Delta)}$
0.1°	TMI	11	9–14	17	13–17
	PR	13	7–15	17	9–14
0.2°	TMI	9	8–11	15	6–17
	PR	10	10–14	15	8–13
0.5°	TMI	8	6–9	15	8–14
	PR	8	6–9	15	7–12
1.0°	TMI	5	6–9	10	8–13
	PR	5	6–8	10	7–11
2.5°	TMI	4	5–8	7	7–12
	PR	4	5–7	7	7–11
5.0°	TMI	4	5–7	7	7–11
	PR	4	5–7	7	6–10

where N is the number of comparisons points in a month or season listed in Table 2, σ_g is the standard deviation of the gauge data, and σ_s is the standard deviation of the satellite data. While B90 and BK03 calculate an error for only unconditional rain rate, (4) and (6) are general equations applicable to all rainfall parameters. Because we are interested in isolating any differences in frequency of rainfall from differences in intensity of rainfall, we choose to calculate an empirical error for percent time-raining, conditional rain rate, and accumulation separately. The range of $\bar{\sigma}_{(\Delta)}$ for these parameters is

provided in Table 3. As with the values based on (4), seasonal empirical errors are larger than monthly empirical errors, and both monthly and seasonal empirical errors decrease with increasing spatial scale for all three rainfall parameters.

The data used for the comparisons in this study are from several different sites throughout the tropical ocean regions and from all times of the year. Thus, rain type, range of values, and spatial and temporal statistics are likely to vary significantly over a month or season. This variability is likely to increase the error estimates based

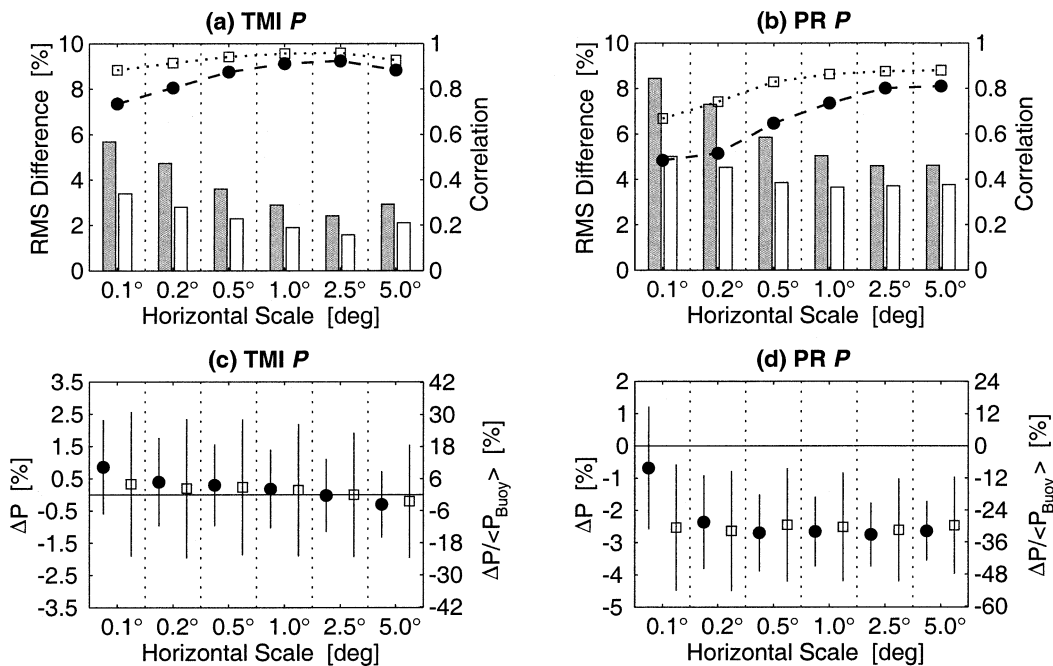


FIG. 3. Rms differences (bars) and correlation coefficients (lines) for percent time-raining comparisons for monthly (filled circles and bars) and seasonal (unfilled squares and bars) data for (a) TMI and (b) PR. Also shown are the mean differences in percent time-raining with respect to the buoys for monthly (circles) and seasonal (squares) data for (c) TMI and (d) PR. Absolute differences are shown on the left vertical axis; relative differences with respect to the mean buoy value are shown on the right vertical axis. The 95% confidence intervals of the mean differences are also shown.

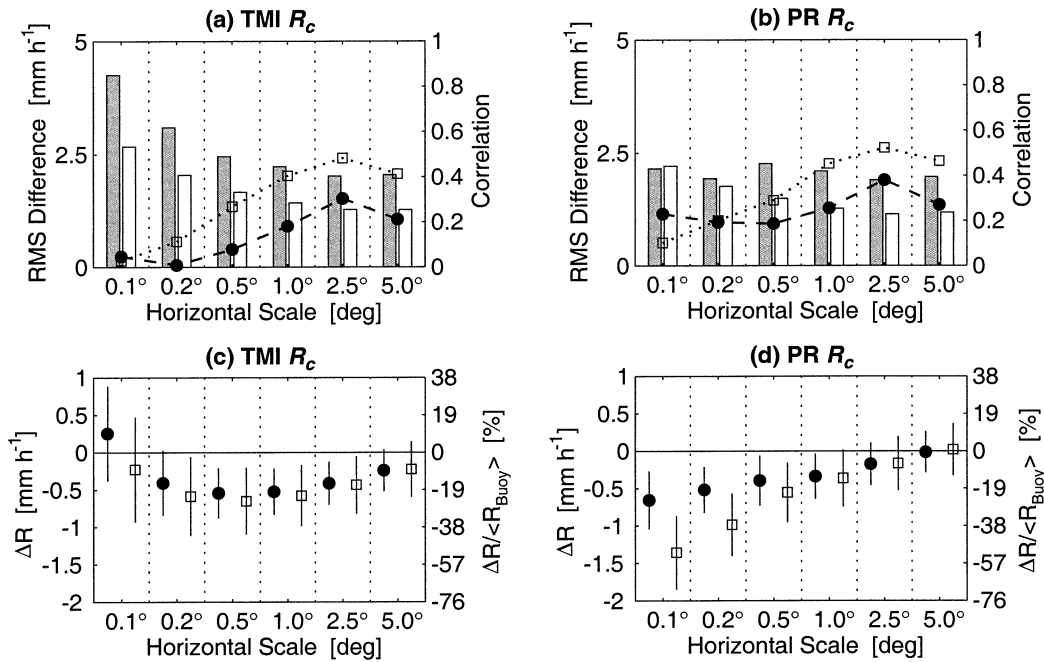


FIG. 4. Same as Fig. 3, but for conditional rain rate.

on (4). Because the empirical errors estimated from (6) are similar to or larger than those estimated from (4), we use the empirical values explicitly in Figs. 3–7 to determine the significance of the mean differences between the buoy and satellite data in this study. We recognize, however, that because of the uncertainties in the input parameters, neither (4) nor (6) provides a perfect estimate of the errors involved in such comparisons.

5. Monthly and seasonal comparisons

a. Comparisons as a function of satellite spatial averaging

Figures 3–5 show TMI and PR percent time-raining, conditional rain rate, and accumulation root-mean-square (rms) differences (bars in Figs. 3a,b, 4a,b, and 5a,b) correlation coefficients (lines in Figs. 3a,b, 4a,b, and 5a,b) and mean differences for all six comparison regions, and for both monthly (filled circles and bars) and seasonal (unfilled squares and bars) timescales. A positive difference indicates that the TRMM values are larger than the buoy values. The left vertical axis in Figs. 3c,d and 4c,d represents the absolute difference, while the right vertical axis represents the difference relative to the buoy mean value. Buoy mean percent time-raining and conditional rain rate are essentially equivalent for the monthly and seasonal data, allowing monthly and seasonal relative differences to be presented on the same axis. The monthly and seasonal buoy mean values for accumulation are not equivalent. Thus, only the relative differences are shown in Figs. 5c and 5d in order to show the monthly and seasonal data on

the same figure. The confidence limits for the differences shown in Figs. 3–5 are determined from the standard error of the mean defined by (6). The 95% confidence limits are roughly 2 times this quantity.

Good agreement between the TMI and buoy percent time-raining is suggested by the results shown in Figs. 3a and 3c. Correlations for these comparisons tend to increase, and rms differences tend to decrease, with increasing spatial scale, with the highest correlations and smallest mean and rms differences being observed for the 2.5° scale for both monthly and seasonal data. On this space scale, the rms difference is 27% of the buoy value for monthly data, and 18% for seasonal data. Based on the squared correlation coefficient, a linear relationship between the buoy and TMI observations explains 85% of the variance for the monthly data, and 92% of the variance for the seasonal data on this scale. There is no significant difference between the TMI and buoy percent time-raining on the 2.5° scale for either monthly or seasonal data.

As with the TMI, PR percent time-raining correlations tend to increase, and rms differences tend to decrease, with increasing spatial scale (Fig. 3b). However, PR correlations are smaller and rms differences are larger than those for the TMI. The PR is equally well correlated with the buoys on both the 2.5° and 5.0° scales for the monthly data, with monthly rms differences also a minimum on these scales. Seasonal correlations are comparable on the 1.0°–5.0° scales, where rms differences are also minimal. In contrast to the TMI, the differences between the PR and buoy values are all significant at the 95% level, with the exception of the monthly 0.1°

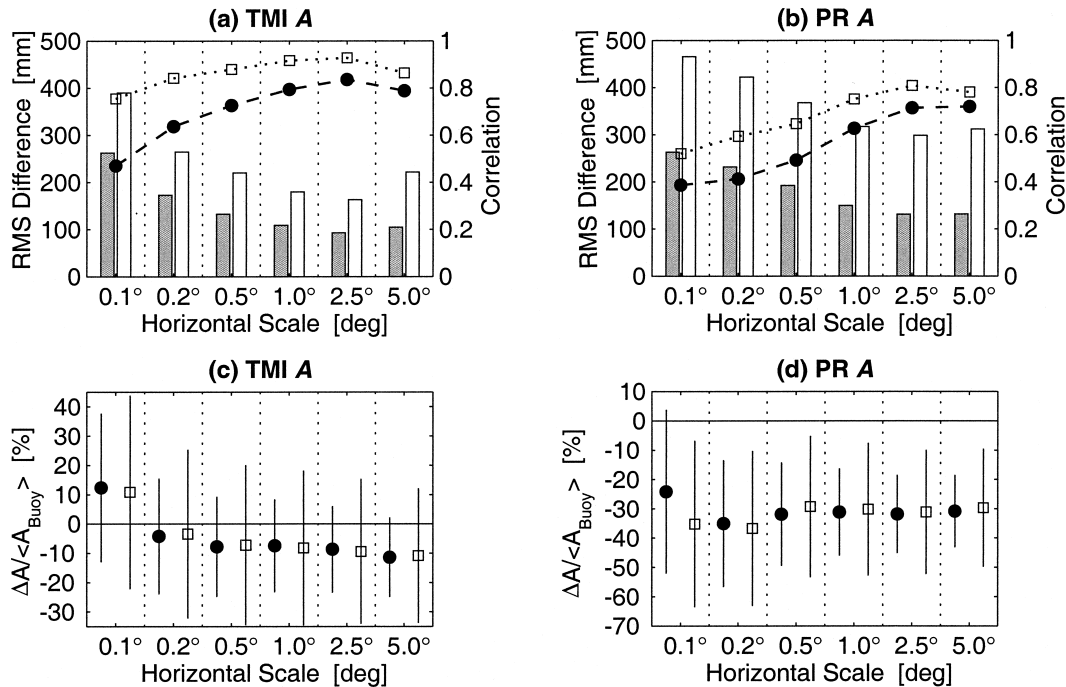


FIG. 5. Same as Fig. 3, but for accumulation. Because mean monthly and seasonal accumulations are not equivalent for this parameter, only relative differences are shown to allow the monthly and seasonal comparisons to be presented on the same axes.

difference (Fig. 3d). However, the correlation of the monthly 0.1° data is only 0.48, calling into question the actual significance of this particular result. The sign of the bias for the 1.0° – 5.0° scales suggests that the PR underestimates the frequency of rain events in comparison with the buoys by about 30%.

The results shown in Fig. 4 indicate that TMI and PR conditional rain-rate comparisons have lower correlations than those for percent time-raining and, for the TMI, higher mean and rms differences. The mean differences indicate that the TMI tends to underestimate conditional rain-rate, in comparison with the buoys, with only the 0.1° and 5.0° mean differences being less than 95% significant for both monthly and seasonal data, and, additionally, the 0.2° mean difference being less than 95% significant for the monthly data (Fig. 4c). Examination of the individual differences between TMI and buoy rain rates reveals that a small mean difference on the 0.1° horizontal scale results from a few large positive differences, skewing the average from an otherwise negative tendency for the differences (data not shown). A similar argument can be made for questioning the results for the 0.2° monthly comparisons. Comparisons for the 5.0° horizontal scale are more highly correlated than for the 0.1° or 0.2° scales, giving more confidence in the results for this scale. The PR seasonal and monthly mean differences are less than 95% significant for the 2.5° and 5.0° regions, and, additionally, the 1.0° region for the seasonal timescale (Fig. 4d).

The highest correlations for both the TMI and PR

monthly and seasonal conditional rain rates are for the 2.5° region. Nevertheless, monthly comparisons explain only 9% of the variance for the TMI and only 14% of the variance for the PR. Similarly, seasonal correlations explain only 23% of the variance for the TMI, and only 27% of the variance for the PR. Monthly rms differences for both TMI and PR are roughly 70% of the buoy mean for this region, reducing to 42% and 47%, respectively, for seasonal comparisons. These values can be compared with those for the percent time-raining comparisons, for which rms differences relative to the buoy means are 27% (18%) for the TMI monthly (seasonal) data and 51% (43%) for the PR monthly (seasonal) data. TMI mean conditional rain-rate differences on this spatial scale are significant at the 95% confidence level and are roughly 15% below the buoy mean value for both monthly and seasonal data, while the PR indicates no significant conditional rain-rate bias with the buoys on either timescale.

Overall, TMI conditional rain rates do not compare as well to the buoys as those from the PR. This can possibly be understood by considering that the PR has a smaller footprint than the TMI and, therefore, better spatial resolution. Thus, despite the fact that the PR has fewer comparison points than the TMI over a month or season, the results in Fig. 4 suggest that the difference in spatial resolution between the PR and TMI footprints is more significant in the comparisons with the buoys, with the buoy measurements more closely resembling

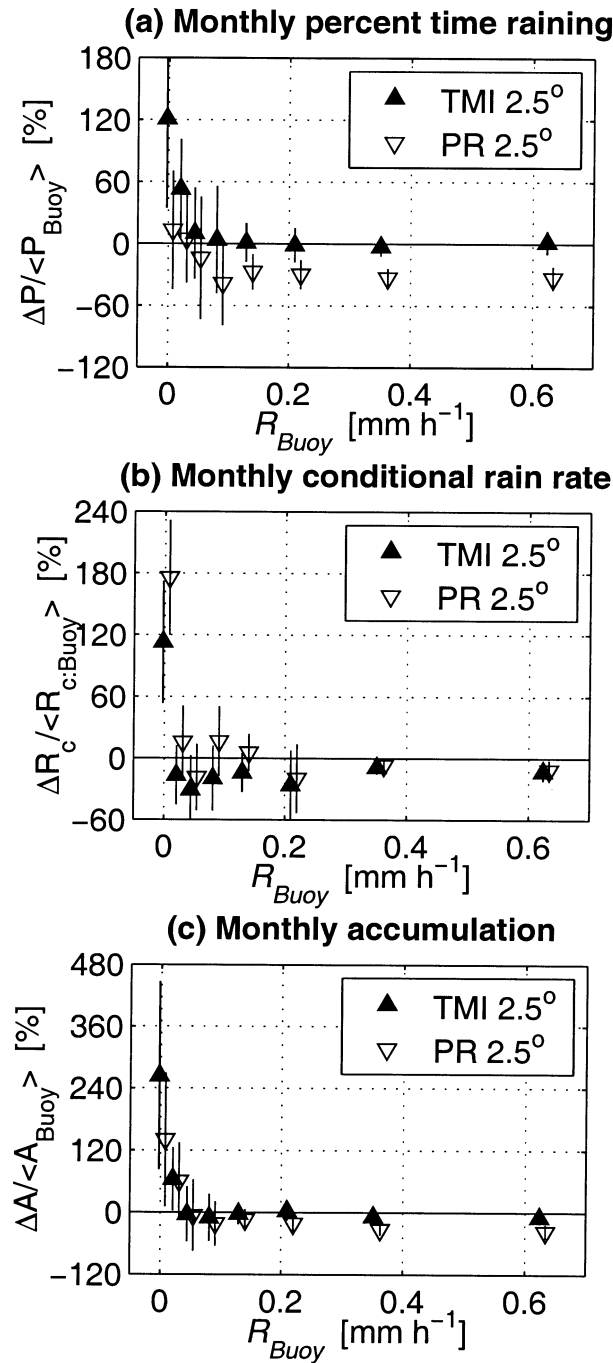


FIG. 6. Monthly 2.5° differences with respect to the buoys for (a) percent time-raining, (b) conditional rain rate, and (c) accumulation for the TMI (filled triangles) and PR (inverted triangles) as a function of rain rate based on the buoy data. TMI values are plotted 0.05 mm h^{-1} to the left of the mean value in each bin, and PR values are plotted 0.05 mm h^{-1} to the right of these values so that points do not overlap.

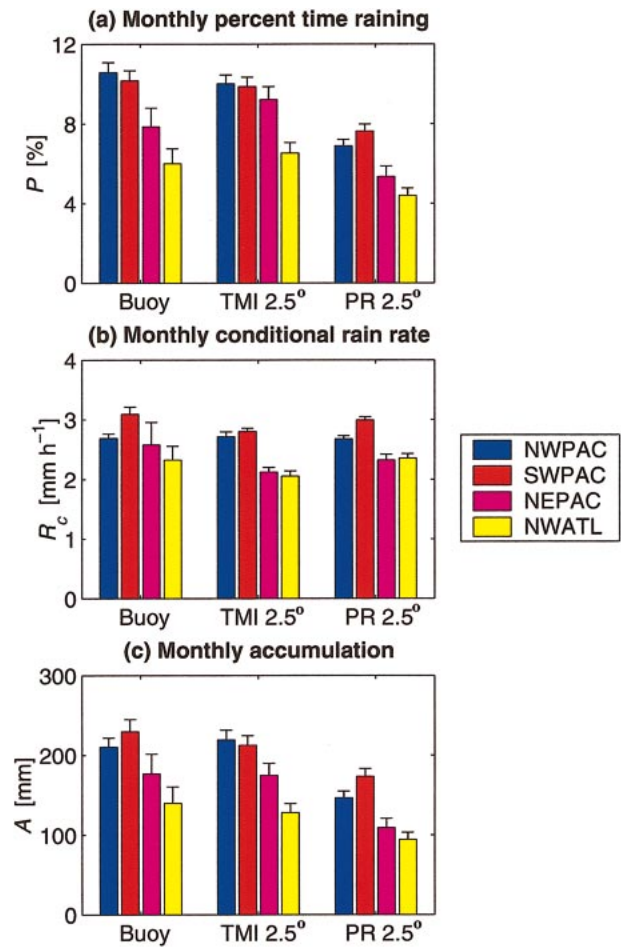


FIG. 7. Monthly (a) percent time-raining, (b) rain rate, and (c) accumulation for the four heavy-rain areas indicated in Fig. 1. Buoy monthly means (bars) and 95% confidence limits (lines above bars) are shown and compared with the monthly 2.5° TMI and PR values.

those of the smaller PR footprint for conditional rain rate.

The TMI and PR accumulation comparisons are generally best for the 2.5° region, for which correlation coefficients are highest, and mean and rms differences are smallest (Fig. 5). In particular, TMI correlations on the 2.5° scale explain 71% of the monthly variance and 86% of the seasonal variance. The corresponding rms differences are about 47% of the buoy mean value for the monthly data and 29% for the seasonal data. While not significant at the 95% confidence level, there is a tendency for the TMI to underestimate rainfall accumulation in comparison with the buoys, with underestimates being about 9% of the buoy value for the 2.5° scale for both monthly and seasonal comparisons.

The best comparisons for the PR are on the 2.5° and 5.0° scales for both monthly and seasonal timescales (Figs. 5b and 5d). Correlations on these scales explain about 50% of the variance for the monthly data, and 66% of the variance for the seasonal data. The corre-

sponding rms differences are about 67% of the buoy mean value for monthly data, and about 55% for seasonal data. Unlike for TMI, all PR mean differences are significant at the 95% confidence level, and indicate that the PR underestimate rainfall accumulation in comparison with the buoys by about 30% for both the monthly and seasonal comparisons.

b. Comparisons as a function of rain rate

A study by Chang and Chiu (2001) found that the TMI compares best with Special Sensor Microwave Imager (SSM/I) data on $5.0^\circ \times 5.0^\circ$ spatial scales for rain rates below 5 mm day^{-1} , above which sampling errors can be greater than $\sim 20\%$. Presumably, sampling errors are more of an issue for the smaller satellite comparison areas used in this study. Having a smaller footprint than the TMI, we expect the PR to also have increased sampling errors for high rain rates, although the Chang and Chiu (2001) study is specific to the TMI. In addition, the results of Bauer et al. (2002) suggest a rain-rate dependence on the TMI retrieval errors. The PR may also have rain-rate-dependent retrieval errors if version 5 of the 2A25 algorithm has less than perfect beam-filling and attenuation corrections (Iguchi et al. 2000).

In order to check our results, as a function of rain rate, we binned the rainfall parameters into eight bins defined by the buoy rain rates and recalculated the mean differences in percent time-raining, conditional rain rate, and accumulation. Because the best comparisons were generally for the $2.5^\circ \times 2.5^\circ$ area, we use 2.5° monthly satellite data for this aspect of the study. There are too few seasonal data comparison points to obtain meaningful statistics as a function of rain rate for these data, so they are not considered. For the monthly data, each bin has on average 30 values that are used to calculate the mean difference and 95% confidence limits. Figure 6 shows the results of these calculations, where the differences have been normalized by the mean buoy value for each bin indicated on the abscissa. As in Figs. 3–5, a positive mean difference indicates the TRMM value is larger than the buoy value.

Starting with percent time-raining, the results shown in Fig. 6a indicate that this value is biased high for TMI and PR at low rain rates, asymptotically approaching nearly the same value as the buoys for the TMI and about 30% below the buoy values for the PR. The asymptotic values are essentially the same as the values of the biases observed in Fig. 3 for the TMI and PR monthly 2.5° data. There is a tendency for the TMI to observe significantly more rain events during months with little or very light rainfall than the PR or buoys. However, as the monthly mean rainfall becomes greater than about 0.1 mm h^{-1} , the TMI and buoys are seen to sample a similar number of rain events. These results are consistent with Bauer et al. (2002), who note that the TMI algorithm has difficulty assigning a rain rate to footprints containing nonprecipitating clouds that are

not part of large precipitating systems, as is likely the case during months with such low monthly rain rates.

Differences in conditional rain rate between the satellite and buoys are also greatest for the lowest rate category, as seen in Fig. 6b. For the TMI, this result is likely due to the fact that the TMI observes more rain events than the buoys for this rate category. Again, it is also possible that the TMI is overestimating the number of precipitating clouds, if sampling errors are accurately represented. The difference between the PR and buoy conditional rain rates imply that the PR rain rates are too high for light-rain events. As with the TMI, however, it is more likely that sampling errors are responsible for the differences between the satellite and buoys for months with so little rain. As seen in Fig. 4, the PR shows better overall agreement with the buoys for conditional rain-rate comparisons than for percent time-raining.

The accumulation differences shown in Fig. 6c are large for months with little or light rainfall, asymptotically approaching the values shown in Figs. 5c and 5d for months with rain rates greater than about 0.1 mm h^{-1} . The tendency for the TMI to overestimate both the frequency and magnitude of light rain in comparison with the buoys results in a significant overestimate of rainfall accumulation when compared with the buoy values for this rain-rate category. Otherwise, the monthly accumulations are close to the buoy values. PR differences in accumulation are significant for all rates except those between about 0.5 and 1.5 mm h^{-1} . Because monthly rain rates of 0.2 – 0.3 mm h^{-1} are about average for the regions in this study, the PR will tend to underestimate the total rainfall when compared with the buoys and TMI, as seen in Fig. 5d.

6. Regional comparisons

The results in section 5b indicate that the TRMM instruments compare well overall to the buoys for the 2.5° horizontal scale and the monthly timescale. Therefore, TRMM data on these scales are used to assess the agreement with the buoys on a regional basis, with regions defined in Fig. 1 and in section 4. Figure 7 shows the monthly 2.5° TRMM values along with the buoy values of percent time-raining, conditional rain rate, and accumulation. The bars are the mean values for each of the four heavy rain areas, and the lines above the bars represent the 95% confidence limits.

All three datasets indicate that percent time-raining is greatest in the western Pacific (NWPAC and SWPAC), with differences significant at the 95% level between this region and the NEPAC and NWATL for the buoy and PR, and between the west Pacific and NWATL for the TMI (Fig. 7a). As expected from the overall comparisons in section 5, the TMI percent time-raining compares well with the buoys, with the exception of the NEPAC region, where the TMI value is 16% higher than the buoy value. Buoy standard deviations

are high in this region, however, such that the differences with the TMI data are not significant at the 95% confidence level. High sampling errors for the buoys result from poor temporal coverage of this particular region for the comparison time period. The PR percent time-raining is underestimated in comparison with the buoys and TMI for all heavy rain areas, similar to the results of the overall comparisons; however, the regional pattern in the frequency of rain events is similar to the other two datasets.

Both the satellite and buoy measurements indicate that rain rates are highest in the NWPAC, with the SWPAC, in particular, having the highest rates for the buoy and PR (Fig. 7b). TMI rain rates are 10% lower than the buoys and 7% lower than the PR in the SWPAC, and 9%–19% lower in the NEPAC and NWATL, consistent with the overall negative bias in TMI rain rates observed in the comparisons shown in Fig. 4. The PR shows overall good agreement with the buoys for all regions, also consistent with the comparisons shown in Fig. 4.

The monthly accumulations indicate that there is more rainfall in the west Pacific (NWPAC and SWPAC) than in the NEPAC or NWATL (Fig. 7c). The buoy and PR results imply that the frequency of rain contributes somewhat more than the intensity of rain to the regional variability in rainfall accumulations, with the range in regional values of percent time-raining being roughly 50%, and the range in regional values of rain rate being about 30%. The TMI results suggest a more equal contribution from both the frequency and intensity of rain events, with the range in percent time-raining being only 40% and the range in rain rates being similar to that of the buoys and PR.

Differences between the TMI and buoy regional accumulations are not significant at the 95% confidence level; however, the best overall agreement is seen for the NWPAC. The PR measures significantly less rainfall than the buoys or TMI in all regions, consistent with the comparisons for this instrument discussed in section 5.

7. Additional concerns

a. Contributions to rainfall from very light rain

While we use 0.5 mm h^{-1} as the minimum rain-rate threshold for the comparisons with the TRMM data, the self-siphoning rain gauges on the buoys are sensitive to accumulation changes as small as 0.15 mm for hourly data. The contribution of rain rates between 0.15 and 0.5 mm h^{-1} to the percent time-raining is about 4% on both monthly and seasonal timescales, increasing the total frequency of rain events measured at the buoys to approximately 13%. The average rain rate, including rain rates between 0.15 and 0.5 mm h^{-1} , decreases from 2.8 to 1.9 mm h^{-1} , as expected, because of the lower threshold on rain rates included in the average. These results combine to increase average accumulations by

4% and 6% for monthly and seasonal data, respectively. The increase in monthly and seasonal accumulations are both within one standard error of the mean values. *Thus, rain rates between 0.15 and 0.5 mm h^{-1} do not contribute significantly to accumulations on these timescales.*

b. The effects of wind-induced errors on the comparisons

Wind-induced undercatchment errors can be substantial for unprotected siphon-type rain gauges, like those deployed on the ATLAS buoys (S01, and references therein). These errors could range anywhere from 10% to 50% for wind speeds typical at the buoy locations analyzed in this study. While there is no wind correction specifically designed for the geometry of the self-siphoning rain gauges on ATLAS buoys, we have applied the correction obtained by Koschmieder (1934) to our rainfall data. This correction is based on several types of siphon gauges at a land site, and for a range of wind speeds comparable to those observed at the buoys.

Using this correction, the buoy monthly percent time-raining increases by 10%, the monthly rain rates increase by 14%, and the monthly accumulations increase by 24%. These increases result in monthly 2.5° TMI mean differences being below buoy values by 6%, 21%, and 22% for percent time-raining, rain rate, and accumulation, respectively. Similarly, monthly 2.5° PR mean differences are below buoy values by 34%, 12%, and 40%, respectively. All TMI and PR differences, with respect to the wind speed-corrected buoy data, are significant at the 95% confidence level. The correlation coefficients for the wind speed-corrected comparisons remain roughly the same as those observed for the uncorrected data, with correlations at small spatial scales showing some improvement over the uncorrected data. Confidence levels also remain roughly the same as those for the uncorrected comparisons, indicating that satellite errors correlated with wind-induced undercatchment errors are not a significant source of the variance in these comparisons. *Because the rain gauges are more than likely to be biased low, these wind-corrected mean differences are likely more realistic estimates of satellite biases.*

8. Conclusions

Rainfall data from self-siphoning rain gauges on open-ocean buoys within the tropical Pacific and Atlantic are compared with TRMM TMI and PR rainfall measurements over a 3-yr time period. Results suggest that the TMI and PR variations in rainfall on monthly and seasonal timescales compare qualitatively well to both the buoys and CMAP rainfall for four heavy-rain areas within these ocean basins. However, the TRMM and buoy monthly values exhibit large differences at times, suggesting that current uncertainties in monthly

precipitation over the tropical open-ocean regions are on the order of the natural variability of rain.

Results of monthly and seasonal comparisons between the TRMM and buoy measurements, using six square areas centered on the buoys for analysis of the satellite data, indicate that TMI and PR satellite data from $2.5^\circ \times 2.5^\circ$ areas centered on the buoys consistently agree well with the buoys on both monthly and seasonal timescales for all three rainfall parameters. On this spatial scale, rms differences in rainfall accumulation are about 47% (29%) for the TMI monthly (seasonal) data relative to the buoy means, and are about 67% (53%) for the PR monthly (seasonal) data. Correlations explain 71% (86%) of the monthly (seasonal) variance for the TMI, and 50% (66%) of the monthly (seasonal) variance for the PR. In addition, no TMI monthly or seasonal mean differences are significant at the 95% confidence level, while all but the 0.1° monthly PR differences are significant at this level and are about 30% less than the buoy values.

Evaluation of these comparisons should be considered in the context of the buoy rain gauges providing a lower bound on rainfall estimates. Buoy data corrected for wind-induced errors increase monthly buoy accumulations by an estimated 24%. Comparisons with these corrected buoy data imply that the 2.5° monthly TMI data underestimate rainfall by about 22%, and 2.5° monthly PR underestimates increase to about 40% below buoy values. These differences are significant at the 95% confidence level calculated from the data variance.

Differences in percent time-raining, conditional rain rate, and, therefore, accumulation, are somewhat dependent on rain rate for both TMI and PR, with the greatest differences observed for months with little or very light rainfall. While sampling errors are suspected to be the reason for these differences, it is also possible that the satellite retrievals are overestimating the intensity of lightly precipitating or nonprecipitating clouds. We are unable to assert which of these explanations is the most likely because of the uncertainty in the estimates of our sampling errors, especially for months with such little rainfall. Differences between the satellite and buoy measurements for months with rain rates greater than about 0.1 mm h^{-1} are in agreement with the overall comparisons. Because sampling errors decrease with increasing rain rate, this implies that the overall comparisons are within the range of rain rates the least affected by sampling errors.

Regional comparisons of monthly 2.5° TRMM data with monthly buoy data indicate that rainfall is more frequent, and somewhat more intense, in the western Pacific than in the northeast Pacific or Atlantic. TMI underestimates of rain rate are found to be largest in the northeast Pacific and Atlantic, while underestimates of percent time-raining and accumulation by the PR are found to be consistent for all regions.

The TRMM objective was to measure $5.0^\circ \times 5.0^\circ$ monthly rainfall with a long-term accuracy of 10%

(Simpson et al. 1996). Results of this study suggest that, for months with greater than 0.1 mm h^{-1} average rainfall, version 5 of the TMI algorithm gives values up to 22% lower than the buoy monthly rainfall, while version 5 of the PR gives values anywhere from 30% to 40% lower than the buoy values. These results assume that satellite–gauge sampling errors, satellite retrieval errors, and wind-induced undercatch by the buoy gauges have been accurately estimated. As estimates of these errors improve, and/or satellite retrieval algorithms and sampling improve, comparisons with the buoys will need to be revisited.

Acknowledgments. The authors thank Sandra Yuter, Tom Bell, and George Huffman for their helpful discussions on comparing satellite and buoy data. We also acknowledge the comments of three anonymous reviewers, which greatly improved the quality of this manuscript. This analysis would not have been possible without the support of the TAO group at NOAA's Pacific Marine Environmental Laboratory. This research is funded by grants from NASA's Tropical Rainfall Measuring Mission and NOAA's Office of Atmospheric and Oceanic Research. This publication is also supported by a grant to the Joint Institute for the Study of the Atmosphere and Ocean (JISAO) under NOAA Cooperative Agreement No. NA17RJ1232.

REFERENCES

- Bauer, P., J.-F. Mahfouf, W. S. Olson, F. S. Marzano, S. D. Michele, A. Tassa, and A. Mugnai, 2002: Error analysis of TMI rainfall estimates over ocean for variational data assimilation. *Quart. J. Roy. Meteor. Soc.*, **128**, 2129–2144.
- Bell, T. L., and P. K. Kundu, 2003: Comparing satellite rainfall estimates with rain-gauge data: Optimal strategies suggested by a spectral model. *J. Geophys. Res.*, **108**, 4121, doi:10.1029/2002JD002641.
- , A. Abdullah, and R. L. Martin, 1990: Sampling errors for satellite-derived tropical rainfall: Monte Carlo study using a space–time stochastic model. *J. Geophys. Res.*, **95**, 2195–2205.
- Chang, A. T. C., and L. S. Chiu, 2001: Non-systematic errors of monthly oceanic rainfall derived from passive microwave radiometry. *Geophys. Res. Lett.*, **28**, 1223–1226.
- Cronin, M. F., N. Bond, C. Fairall, J. Hare, M. J. McPhaden, and R. A. Weller, 2002: Enhanced oceanic and atmospheric monitoring for the Eastern Pacific. *EOS, Trans. Amer. Geophys. Union*, **83**, 205, 210–211.
- Groisman, P. Y., and D. R. Legates, 1994: The accuracy of United States precipitation data. *Bull. Amer. Meteor. Soc.*, **75**, 215–227.
- Iguchi, T., T. Kozu, R. Meneghini, J. Awaka, and K. Okamoto, 2000: Rain-profiling algorithm for the TRMM precipitation radar. *J. Appl. Meteor.*, **39**, 2038–2052.
- Kedem, B., L. S. Chiu, and G. R. North, 1990: Estimation of mean rain rate: Application to satellite observations. *J. Geophys. Res.*, **95**, 1965–1972.
- Koschmieder, H., 1934: Methods and results of definite rain measurements. *Mon. Wea. Rev.*, **62**, 5–7.
- Kummerow, C., W. Barnes, T. Kozu, J. Shiue, and J. Simpson, 1998: The Tropical Rainfall Measuring Mission (TRMM) sensor package. *J. Atmos. Oceanic Technol.*, **15**, 809–817.
- McPhaden, M. J., 1999: Genesis and evolution of the 1997–98 El Niño. *Science*, **283**, 950–954.
- , and Coauthors, 1998: The Tropical Ocean-Global Atmosphere

- observing system: A decade of progress. *J. Geophys. Res.*, **103**, 14 169–14 240.
- Schumacher, C., and R. A. Houze Jr., 2000: Comparison of radar data from the TRMM satellite and Kwajalein oceanic validation site. *J. Appl. Meteor.*, **39**, 2151–2164.
- Serra, Y. L., P. A. Hearn, P. Freitag, and M. J. McPhaden, 2001: ATLAS self-siphoning rain gauge error estimates. *J. Atmos. Oceanic Technol.*, **18**, 1980–2001.
- Servain, J., A. J. Busalacchi, M. J. McPhaden, A. D. Moura, G. Reverdin, M. Vianna, and S. E. Zebiak, 1998: A Pilot Research Moored Array in the Tropical Atlantic (PIRATA). *Bull. Amer. Meteor. Soc.*, **79**, 2019–2031.
- Simpson, J., C. Kummerow, W.-K. Tao, and R. F. Adler, 1996: On the Tropical Rainfall Measuring Mission (TRMM). *Meteor. Atmos. Phys.*, **60**, 19–36.
- U.S. Department of Commerce, 2002: Climate Diagnostics Bulletin. No. 01/12, 89 pp.
- Xie, P., and P. A. Arkin, 1997: Global precipitation: A 17-year monthly analysis based on gauge observations, satellite estimates, and numerical model outputs. *Bull. Amer. Meteor. Soc.*, **78**, 2539–2558.